Taylor & Francis
Taylor & Francis Group

RESEARCH PAPER

Check for updates

KLF2-induced circZKSCAN1 potentiates the tumorigenic properties of clear cell renal cell carcinoma by targeting the miR-1294/PIM1 axis

Mingzi Li[a], Mingxun Zhang[b,c,*], Muling Chen[a], Jiantao Xiao[d], Xingyu Mu[a], Jingtao Peng[e], and Jie Fan[a]

[a]Department of Urology, Shanghai General Hospital, School of Medicine, Shanghai Jiaotong University, Shanghai, Shanghai, China; [b]Department of Pathology, the First Affiliated Hospital of Ustc, Division of Life Sciences and Medicine, University of Science and Technology of China, Hefei, Anhui, China; [c]Intelligent Pathology Institute, Division of Life Sciences and Medicine, University of Science and Technology of China, Hefei, Anhui, China; [d]Department of Urology, Zhongnan Hospital of Wuhan University, Wuhan, Hubei, China; [e]Department of Urology, Union Hospital, Tongji Medical College, Huazhong University of Science and Technology, Wuhan, Hubei, China

ABSTRACT

Clear cell renal cell carcinoma (ccRCC) is one of the most common and lethal types of urologic cancer. With low survival rates among patients in advanced stages of disease, and increasing rate of morbidity and mortality worldwide, novel therapeutic targets for ccRCC clinical intervention are necessary. In this study, we investigated the functional role of circZKSCAN1 in ccRCC progression. Our results suggested that circZKSCAN1 was abundantly expressed in ccRCC tumor tissues and cells. CircZKSCAN1 knockdown significantly inhibited cell proliferation, migration, invasion, and epithelial-to-mesenchymal transition of renal cell carcinoma (RCC) cells, whereas potentiated Natural Killer (NK) cell-mediated cytotoxicity against RCC cells *in vitro* and repressed tumor growth *in vivo*. Furthermore, we identified a novel circZKSCAN1/miR-1294/PIM1 axis was identified in RCC progression, showing that the expression of circZKSCAN1 expression in RCC cells was transcriptionally regulated by Kruppel-like factor 2. The results of our study may provide new insights for ccRCC basic research.

Abbreviations: ccRCC: clear cell renal cell carcinoma; ChIP: chromatin immunoprecipitation; circRNA: circular RNA; EDU: 5-ethynyl-2′-deoxyuridine; EMT: epithelial-mesenchymal transition; FBS: fetal bovine serum; FISH: RNA fluorescent in situ hybridization; KLF2: Kruppel-like factor 2; NC: normal control; NK cell: natural killer cell; NOD/SCID: nonobese severe diabetic/severe combined immunodeficiency; PIM1: Pim-1 proto-oncogene, serine/threonine kinase; RCC: renal cell carcinoma; ZKSCAN1: zinc finger with KRAB and SCAN domains 1

Introduction

Renal cell carcinoma (RCC) is one of the most common types of malignant urologic cancers, accounting for approximately 3% of malignant neoplasia and 90% of renal malignancies [1,2]. Clear cell renal cell carcinoma (ccRCC) comprises about 80% to 90% of RCCs, with higher morbidity and relapse rates than other subtypes of RCCs [3]. Nearly 30% of patients are diagnosed with ccRCC at an advanced stage when the survival time is rather short [4]. Although advancements in the clinical management of ccRCC has been made, including surgery, radiotherapy, chemotherapy, and gene therapy, the outcomes of ccRCC patients remains poor [5,6]. Identification of novel

diagnostic and therapeutic targets for ccRCC is urgently demanded.

Circular RNAs (circRNAs) are a subtype of non-coding RNAs with a special circular, covalently bonded structure. With the innovations in RNA sequencing (RNA-seq) technologies and bioinformatics, accumulating circRNAs have been identified in the past two decades [7–9]. The molecular mechanisms and biological functions of circRNAs have recently been studied in-depth regarding the conservation, abundance, and tissue specificity features [10]. Mechanistically, multiple functions have been verified for circRNAs, such as acting as competing endogenous RNAs or miRNA sponges [11],

---

CONTACT Jie Fan ✉ Jief67@sina.com 🔾 Department of Urology, Shanghai General Hospital, School of Medicine, Shanghai Jiaotong University, Shanghai, China

*Co-first authors

ⓘ Supplemental data for this article can be accessed here.

interacting with proteins [12,13], modulating mRNAs stability [14,15], regulating gene transcription [16], and even translating proteins [17]. Biologically, circRNAs are involved in a number of cellular progression events, such as proliferation [18], apoptosis [19], migration [20], invasion [21], and angiogenesis [22]. Currently, circRNAs are treated as a promising therapeutic target for various diseases.

Emerging evidence supports an important role of circRNAs in ccRCC progression. Xue D et al demonstrated that circ-AKT3 suppresses ccRCC progression by modulating miR-296-3p/ E-cadherin signals [23]. Chen Z et al found a novel hsa_circ_001895/miR-296-5p/SOX12 axis in ccRCC development [24]. Han B et al revealed the function of circHIPK3/miR-508-3p/ CXCL13 signal in ccRCC tumorigenesis progression [25]. Circular RNA Zinc Finger with KRAB and SCAN Domains 1 (circZKSCAN1) has been shown to participate in the progression of multiple cancers. Bi J et al showed that circZKSCAN1 inhibits bladder cancer progression through the miR-1178-3p/P21 axis [26]. Wang Y et al demonstrated a functional role for the circZKSCAN1/miR-330-5p/FAM83A axis in non-small cell lung cancer [27]. Moreover, the investigations of both circZKSCAN1 and its linear form in hepatocellular progression have been well documented [28,29]. However, the role of circZKSCAN1 in ccRCC progression remains unstudied.

In this study, we hypothesized that circZKSCAN1 plays a function in ccRCC development. First, the characterization and expression of circZKSCAN1 in ccRCC were demonstrated. Next, using cell and animal models, we investigated the biological function of circZKSCAN1 in ccRCC tumorigenesis. Subsequently, we identified a novel circZKSCAN1/miR-1294/PIM1 axis in ccRCC progression by conducting a serial experiment. Finally, we found that circZKSCAN1 levels were transcriptionally mediated by Kruppel-like factor 2 (KLF2) in ccRCC cells. Our results may provide a new insight for ccRCC basic research.

Materials and methods

Human samples

A total forty pairs of ccRCC tissues were collected from untreated patients who with no metastasis at the urology center, Shanghai General Hospital, from August 2012 to December 2013. All tissues samples were harvested in a healthy (5 cm from the tumor) and at a tumor-affected region from each patient. The pathological diagnosis of each sample was independently confirmed by two pathologists. We obtained informed consent from all patients before the study. All procedures involving human samples were approved by the ethics committee of the Shanghai General Hospital.

Cell culturing and transfection

The cells used in this study were obtained from the American Type Culture Collection. ccRCC cells were cultivated in RPMI 1640 medium supplied with 10% fetal bovine serum (FBS), and 293 T cells were cultivated in DMEM with 10% FBS. We performed transfection using Lipofectamine 3000 or RNAiMax Transfection Reagent (Invitrogen) following the manufacturer's protocol. The normal control (NC), specific siRNAs for circZKSCAN1, lentivirus for PIM1, and miR-1294 mimics were purchased from GenePharma (Shanghai, China). The information on the sequences is provided in Supplementary Table 1.

Quantitative Reverse Transcription PCR (qRT-PCR)

Total RNAs from cells and tissues were isolated with TRIzol reagent (Invitrogen) following the manufacturer's protocol. The Superscript RT Kit (TOYOBO) was used to perform the reverse transcription process, and the SYBR Green PCR Master Mix Kit (TOYOBO, Japan) was used to conduct quantitative PCR following the manufacturer's protocols. Endogenous glyceraldehyde 3-phosphate dehydrogenase (GAPDH) and U6 were used as internal controls. The primers used

in this study are provided in Supplementary Table 2.

RNA Fluorescent In Situ Hybridization (FISH)

The cellular distribution of circZKSCAN1 in ACHN and CAKI-1 cells was detected using the FISH kit (Ribibio, China) following the manufacturer's protocol. Pre-hybridization solutions were added to the culture medium of ACHN and CAKI-1 cells for 30 minutes of incubation; then, 20 μM of hybridization solution was added to probes and hybridized for 12 hours. The slides obtained were washed with saline sodium citrate three times and then subjected to DAPI staining. The results were visualized and recorded by confocal microscopy.

Western blot

First, all cells were lysate and added with SDS-PAGE buffer. After that, the proteins harvested were electronically transferred onto nitrocellulose membranes (GE Healthcare). Low-fat milk (5%) was used to block the membranes, which were next washed three times using TBS-T. In the next step, membranes were incubated with primary antibodies, followed by secondary antibodies. The results were photographed using the ECL Chemiluminescence System (Santa Cruz). The antibodies used in this study are described in Supplementary Table 3.

5-Ethynyl-2′-Deoxyuridine (EDU) assay

We used the Cell-Light EdU DNA Cell proliferation kit (RiboBio, China) to evaluate cell proliferation levels according to the manufacturer's guide. Briefly, cells were seeded and cultured for 48 to 72 hours and added with 50 mM EdU for another 2 hours. Cell's nucleic acids were stained with DAPI solution, and cells were fixed by Apollo Dye Solution. The Image J software (NIH, USA) was used to analyze cell proliferation levels.

Transwell assay

A transwell assay was performed using an 8 μm polycarbonate membrane (Corning, US) and 1 μg/μl Matrigel basement membrane matrix (BD Biosciences, US) to assess the cell migration and invasion levels. In summary, the upper chamber was filled with 100 μl of serum-free media, whereas the lower chamber was filled with 600 μl DMEM with 10% of FBS. Cells were seeded and cultured for 12 hours, and all membranes in chambers were added with crystal violet and photographed upon a microscope. All experiments were conducted in triplicate, followed by results analysis.

Measurements of Natural Killer (NK) cell-mediated cytotoxicity

Measurements of NK cell-mediated cytotoxicity were performed following a protocol previously published [30]. Briefly, NK cell cytotoxicity toward transfected RCC cells was evaluated by calcein release assays using 30 μM of calcein-AM (Dojindo) in 20/40/60 E/T radios. A perforin polarization assay was conducted to score the numbers of NK cells contacting RCC-transfected cells. In addition, a conjugation assay was performed to evaluate the conjugate formation between NK cells and RCC-transfected cells.

RNA pull-down

Biotinylated circZKSCAN1, miR-1294, and control probes were obtained from GeneChem (Shanghai, China). Briefly, cells were lysed and added a co-immunoprecipitation buffer (Beyotime, China), with the assay set for high amplitude performance. Next, circZKSCAN1 or miR-1294 probe-streptavidin beads (Life, USA) were added to cell lysates for overnight incubation. The RNA isolation was performed using TRIzol (Invitrogen, US), and results were analayzed by qRT-PCR.

Chromatin immunoprecipitation (ChIP)

The EpiQuik Chromatin Immunoprecipitation Kit (Epigentek, NY, USA) was used to assess the occupation of KLF2 on the ZKSCAN1 promoter according to the manufacturer's protocol. Briefly, ACHN and CAKI-1 cell lysates were collected and added with 1% formaldehyde for 10 minutes and then quenched with glycine. Subsequently, treated lysates

were sonicated and incubated overnight with KLF2 or IgG antibodies at 4°C. After that, the lysates were incubated with protein A agarose for 1 hour. The bound fragments were subjected to PCR assay.

Dual-luciferase reporter assay

The wide-type or mutant sequences of miR-1294 were harbored into PmirGLO vectors (Promega, USA). Next, luciferase reporter vectors were co-transfected with miR-1294 mimics into cells. Results were tested by a Dual-Luciferase Reporter Assay System (Promega, US).

Xenografts in mice

Six-week-old nonobese severe diabetic/severe combined immunodeficiency (NOD/SCID) mice (n = 30) were kept in 2 separate groups (n = 5 per group). Transfected ACHN cells (1×10^6 cells for each tumor) were subcutaneously inoculated into NOD/SCID mice. Tumor volumes were recorded four days a time and repeated seven times. Four weeks later, mice were sacrificed, and tumors were isolated. The animal study was approved by the Committee for Animal Care and Use of the Shanghai General Hospital.

Statistical analysis

Statistical analysis of experimental data was conducted using the SPSS (Statistical Package for the Social Sciences; IBM, USA) software version 19.0. The Student t test was used to test the differences between 2 groups, whereas one-way analyses of variance were conducted to compare 3 or more groups. Expression correlations between circZKSCAN1, miR-1294, and PIM1 were calculated by Spearman analyses. All experiments within this study were performed in triplicate unless otherwise stated. Results are shown as mean ± SD, and P values lower than .05 suggest statistical significance.

Results

Characteristics of circZKSCAN1 in ccRCC

First, we measured the expression of circZKSCAN1 (Figure 1(a)) in ccRCC cell lines; circZKCAN1 expression was generally upregulated, especially in ACHN and CAKI-1 cells (Figure 1(b)). After that, we characterized the circular RNA of circZKSCAN1 in ccRCC cell lines. Reverse transcription experiments showed that circZKSCAN1 expression was lower than ZKSCAN1 expression when oligo (dT)18 primers were used in ACHN (Figure 1(c)) or CAKI-1 (Figure 1(d)) cells. Upon transcription inhibitor actinomycin D treatment, circZKSCAN1 had a longer half-life than ZKSCAN1 in ACHN (Figure 1(e)) or CAKI-1 (Figure 1(f)) cells, suggesting that circZKSCAN1 is more stable than ZKSCAN1 in ccRCC cells. Moreover, circZKSCAN1 was more resistant to RNase R digestion than ZKSCAN1 in ACHN (Figure 1(g)) and CAKI-1 (Figure 1(h)) cells, indicating that circZKSCAN1 is in its circular form. The intracellular fraction assay in ACHN (Figure 1(i)) or CAKI-1 (Figure 1(j)) and the RNA-FISH assay (Figure 1(k)) showed that circZKSCAN1 was mainly distributed in the cytoplasm. CircZKSCAN1 expression in ccRCC tumor tissues was significantly higher than in normal tissues (Figure 1(l)). These results indicated that circZKSCAN1 was upregulated in ccRCC and might be involved in ccRCC progression.

CircZKSCAN1 knockdown inhibits ccRCC cell malignancy and potentiates NK cell-mediated cytotoxicity

To investigate the biological function of circZKSCAN1 in ccRCC, we generated circZKSCAN1 knockdown cell models. Upon siRNAs treatment, circZKSCAN1 expression, but not ZKSCAN1 expression, was significantly decreased in ACHN and CAKI-1 cells (Figure 2(a)). Results of EDU and transwell assays showed that circZKSCAN1 knockdown significantly inhibited cell proliferation (Figure 2(b,c)), migration (Figure 2(d,e)), and invasion (Figure 2(f,
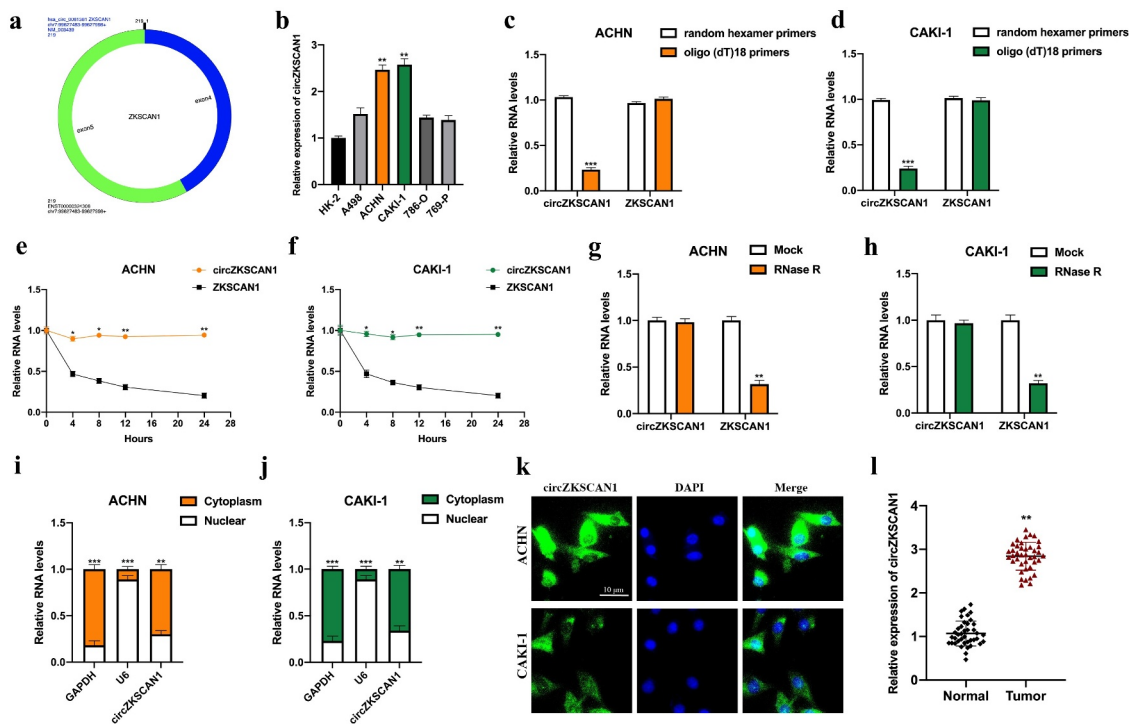
Figure 1. The characteristics of circZKSCAN1 in ccRCC. A: A schematical illustration of circZKSCAN1 is shown. B: CircZKSCAN1 expression in ccRCC cell lines was measured by qRT-PCR. C-D: Reverse transcription assays were performed using Random hexamer or oligo (dT)18 primers in ACHN (c) or CAKI-1 (d) cells; results were calculated by qRT-PCR. E-F: CircZKSCAN1 expression in ACHN (e) and CAKI-1 (f) upon actinomycin D treatment were measured at the indicated time points. G-H: Expression levels of circZKSCAN1 in ACHN (g) and CAKI-1 (h) after RNase R digestion were measured. I-J: CircZKSCAN1 distribution in ACHN (i) and CAKI-1 (j) cells were assessed by an intracellular fraction. K: circZKSCAN1 location in ACHN and CAKI-1 were detected by RNA-FISH assay. L: Expression levels of circZKSCAN1 in the forty pairs of ccRCC tissues were detected by qRT-PCR. Experiments were conducted in triplicate. Data are presented as mean ± SD. *$P < 0.05$, **$P < 0.01$, ***$P < 0.001$.

g)). Epithelial-to-mesenchymal transition (EMT)-related protein expression (E-cadherin, N-cadherin, Vimentin, MMP-2, and MMP-9) was detected in circZKSCAN1 knockdown cells, as shown in Figure 2(h-J), and its knockdown reduced EMT in ccRCC cells. In addition, we assessed the effect of circZKSCAN1 on RCC cells' susceptibility to NK cells. The calcein release assay (Figure 2(k)), perforin polarization (Figure 2(l)), and conjugation assays (Figure 2(m,n)) showed that circZKSCAN1 knockdown markedly potentiated the NK cell-mediated cytotoxicity toward RCC cells. Moreover, by constructing mouse xenografts using si-circZKSCAN1-transfected ACHN cells, we showed that circZKSCAN1 knockdown inhibited tumor growth *in vivo* (Figure 2(o-q)). Therefore, these results indicated that circZKSCAN1 plays an oncogene role in ccRCC development.

CircZKSCAN1 sponges miR-1942

Bioinformatics analyses (ENCORI: http://starbase. sysu.edu.cn) with high stringency (≥3) CLIP Data and low stringency (≥1) Degradome Data were performed to find putative miRNAs targets for circZKSCAN1 (Figure 3(a)). Subsequently, biotinylated RNA pull-down using bio-circZKSCAN1 probes was conducted to evaluate the possible association between circZKSCAN1 and putative miRNAs in ACHN (Figure 3(b)) and CAKI-1 (Figure 3(c)) cells, miR-1178-3p as positive control [26]. Results analyzed by qRT-PCR suggested that circZKSCAN1 might sponge miR-1294. The expression of miR1294 was significantly upregulated in ACHN (Figure 3(d)) and CAKI-1 (Figure 3(e)) cells upon circZKSCAN1 knockdown. We synthesized the predicted binding sites between circZKSCAN1 and miR-1294 (Figure 3(f)). The association between
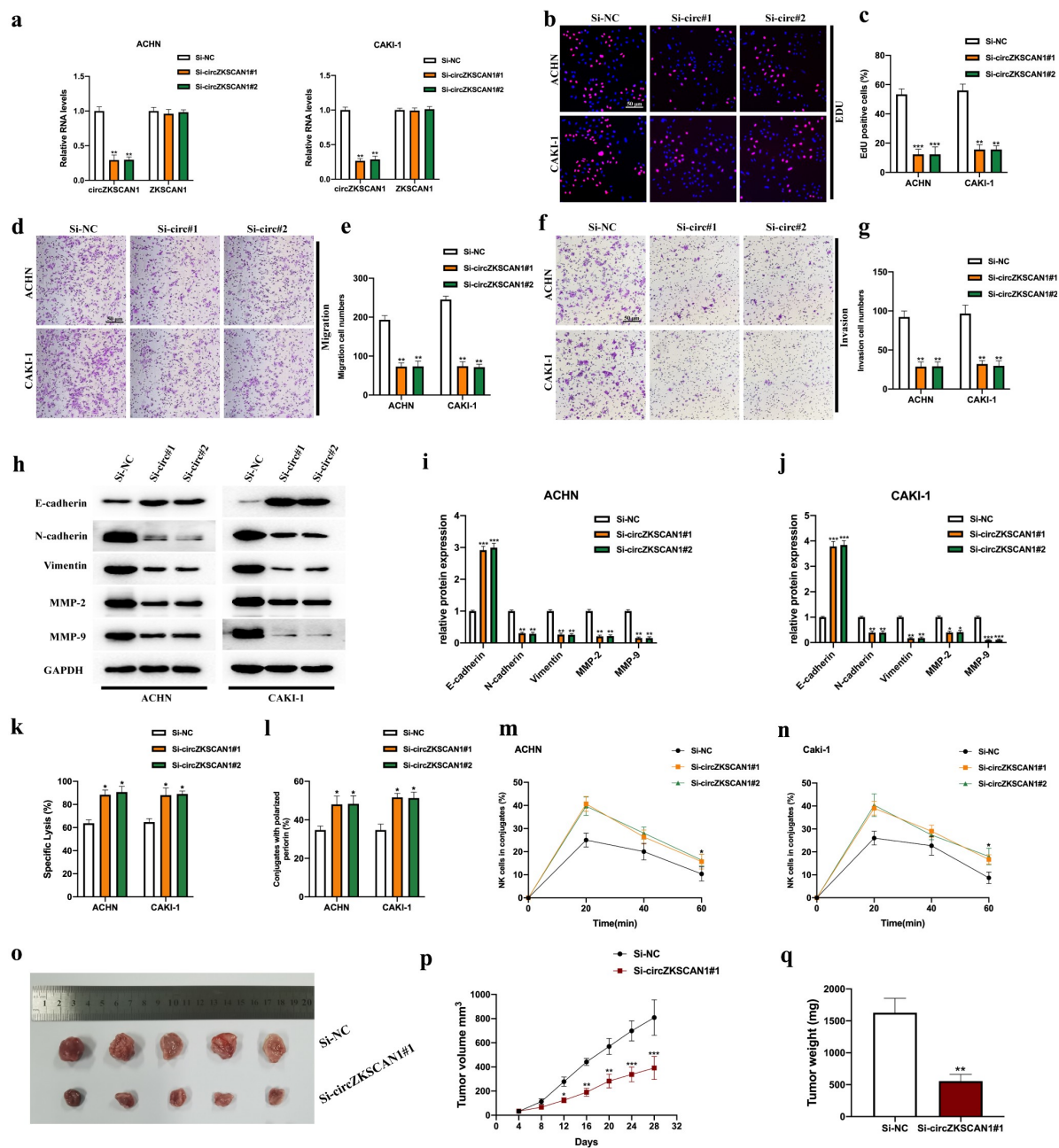
Figure 2. CircZKSCAN1 knockdown inhibits ccRCC cell malignancy and potentiates NK cell-mediated cytotoxicity. A: CircZKSCAN1 knockdown cell models were generated by introducing si-NC, si-circZKSCAN1#1, and si-circZKSCAN1#2 into ACHN and CAKI-1 cells, and the expression levels of circZKSCAN1 or ZKSCAN1 in cells were detected. B-C: Cell proliferation level was detected by EDU assays (b); the statistical calculation is presented (c). D-E: Cell migration level was measured by transwell migration assays (d), and results were recorded (e). F-G: The invasion levels of transfected cells were detected using transwell invasion assays (f); statistically significant results are shown (g). H-J: EMT-related proteins were measured by western blot (h), and results were analyzed (i-j). NK cell-mediated cytotoxicity was assessed by calcein release (k), perforin polarization (l), and conjugation assays (m-n), as indicated. O: The inoculated tumors are presented and quantified by volume (p). (q) The tumor end weight results showed that si-circZKSCAN1#1 pre-treated cell produce smaller tumors (n = 5 per group). Experiments were performed in triplicate. Data are presented as mean ± SD. *$P < 0.05$, **$P < 0.01$, ***$P < 0.001$.

circZKSCAN1 and miR-1294 was determined by dual-luciferase reporter assay in 293 T (Figure 3(g)), CAKI-1 (Figure 3(h)), and ACHN (Figure 3(i)) cells. MiR-1294 expression levels were decreased in the forty pairs of ccRCC tumor tissues compared with the adjacent normal tissues (Figure 3(j)) and statistically correlated with circZKSCAN1 expression (Figure 3(k)).
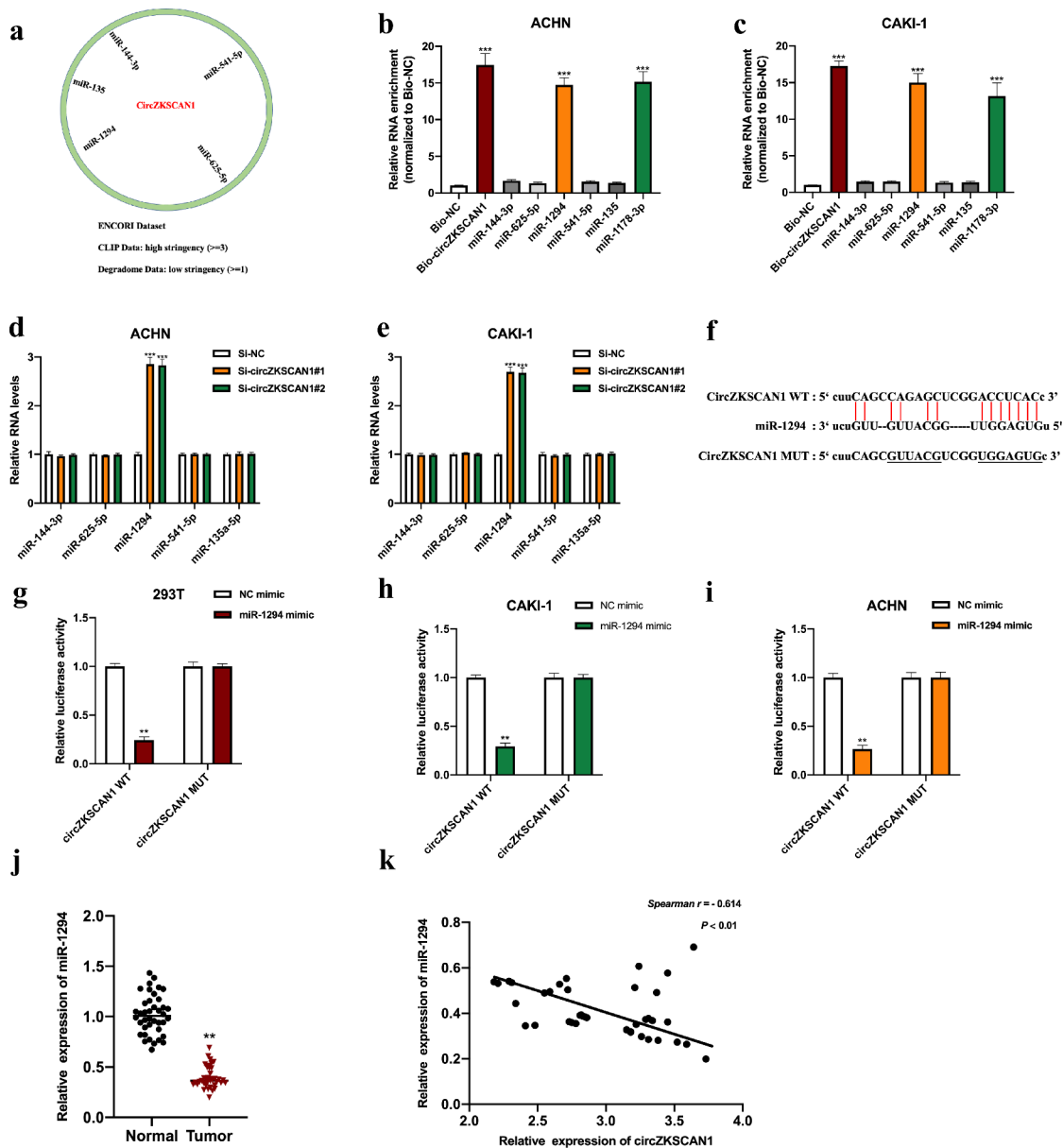
Figure 3. CircZKSCAN1 sponges miR-1942. A: Putative miRNA targets were predicted by bioinformatics analysis. B-C: A biotinylated RNA pull-down assay was conducted to assess the potential miRNA targets enrichment in ccRCC cells; experiment results were analyzed by qRT-PCR. D-E: Putative miRNA targets expressed after circZKSCAN1 knockdown in ACHN (d) or CAKI-1 (e) cells were detected by qRT-PCR. F: Predicted binding sequences between circZKSCAN1 and miR-1294 are shown. G-I: The relationship between circZKSCAN1 and miR-1294 was detected using a dual-luciferase reporter assay in 293 T (g), ACHN (h), and CAKI-1 (i) cells. J: MiR-1294 expression in the forty pairs of ccRCC tissues was detected using the qRT-PCR assay. K: Expression associations between circZKSCAN1 and miR-1294 were calculated by Spearman analysis. Experiments were performed in triplicate. Data are presented as mean ± SD. $*P < 0.05$, $**P < 0.01$, $***P < 0.001$.

MiR-1942 overexpression suppresses ccRCC cell malignancy and potentiates NK cell-mediated cytotoxicity

The role of miR-1294 in ccRCC cellular progression was explored by generating cell models overexpressing miR-1294 (Figure 4(a)). By using EDU and transwell assays, we found that miR-1294 overexpression suppressed ccRCC cell proliferation (Figure 4(b,c)), migration (Figure 4(d,e)), and invasion (Figure 4(f,g)) levels. Furthermore, EMT-related proteins expression was detected, and miR-1294 overexpression significantly decreased EMT in ccRCC cells (Figure 4(h-j)). In addition, miR-1294 overexpression markedly
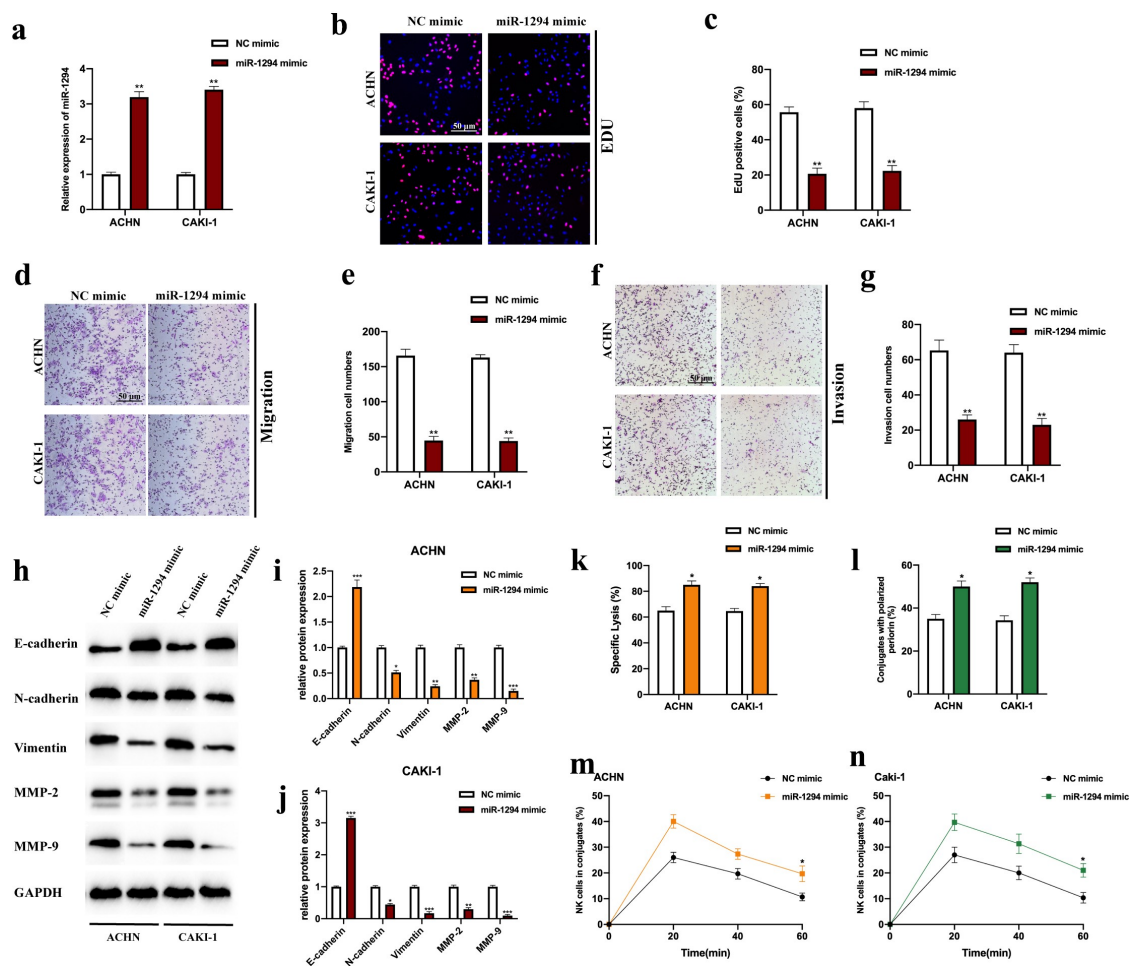
Figure 4. MiR-1942 overexpression suppresses ccRCC cell malignancy and potentiates NK cell-mediated cytotoxicity. A: miR-1294 overexpression cell models were constructed by transfecting NC mimic or miR-1294 mimic into ACHN or CAKI-1 cells; transfection efficiency was detected by qRT-PCR. B-C: an EDU assay (b) was performed to detect cell proliferation levels (c). D-E: Transwell migration experiments (d) were used to detect the migration levels of transfected cells; experiments data were recorded and analyzed (e). F-G: A transwell invasion experiment was performed to assess the invasion levels of transfected cells (f); statistically significant results are shown (g). H-J: Western blot was performed to measure EMT-related protein levels (h), and results were analyzed (i-j). NK cell-mediated cytotoxicity was assessed by conducting calcein release assay (k), perforin polarization assay (l), and conjugation assays (m-n), as indicated. Experiments were conducted three times. Data are presented as mean ± SD. *$P < 0.05$, **$P < 0.01$, ***$P < 0.001$.

aggravated the NK cell-mediated cytotoxicity toward RCC cells (Figure 4(k-n)). From these results, we concluded that miR-1294 plays an essential role in ccRCC progression.

PIM1 is a downstream target for miR-1942

By using the PITA (https://genie.weizmann.ac.il/pubs/mir07/mir07_data.html), MicroT (http://diana.imis.athena-innovation.gr/), and PicTar (https://pictar.mdc-berlin.de/) databases with strict stringency (≥5) CLIP Data and medium stringency (≥2)

Degradome Data, four putative mRNA targets were found, as indicated in Figure 5(a). Biotinylated RNA pull-down assays showed that PIM1 significantly enriched in bio-probes in ACHN (Figure 5(b)) and CAKI-1 (Figure 5(c)) cells. PIM1 expression could be negatively regulated by miR-1294 in ACHN (Figure 5(d)) and CAKI-1 (Figure 5(e)) cells. The predicted binding sites between miR-1294 and PIM1 are shown in Figure 5(f). The interaction was demonstrated by dual-luciferase reporter assay in ACHN (Figure 5(g)), CAKI-1 (Figure 5(h)), and 293 T (Figure 5i) cells. Four pairs of ccRCC tissues
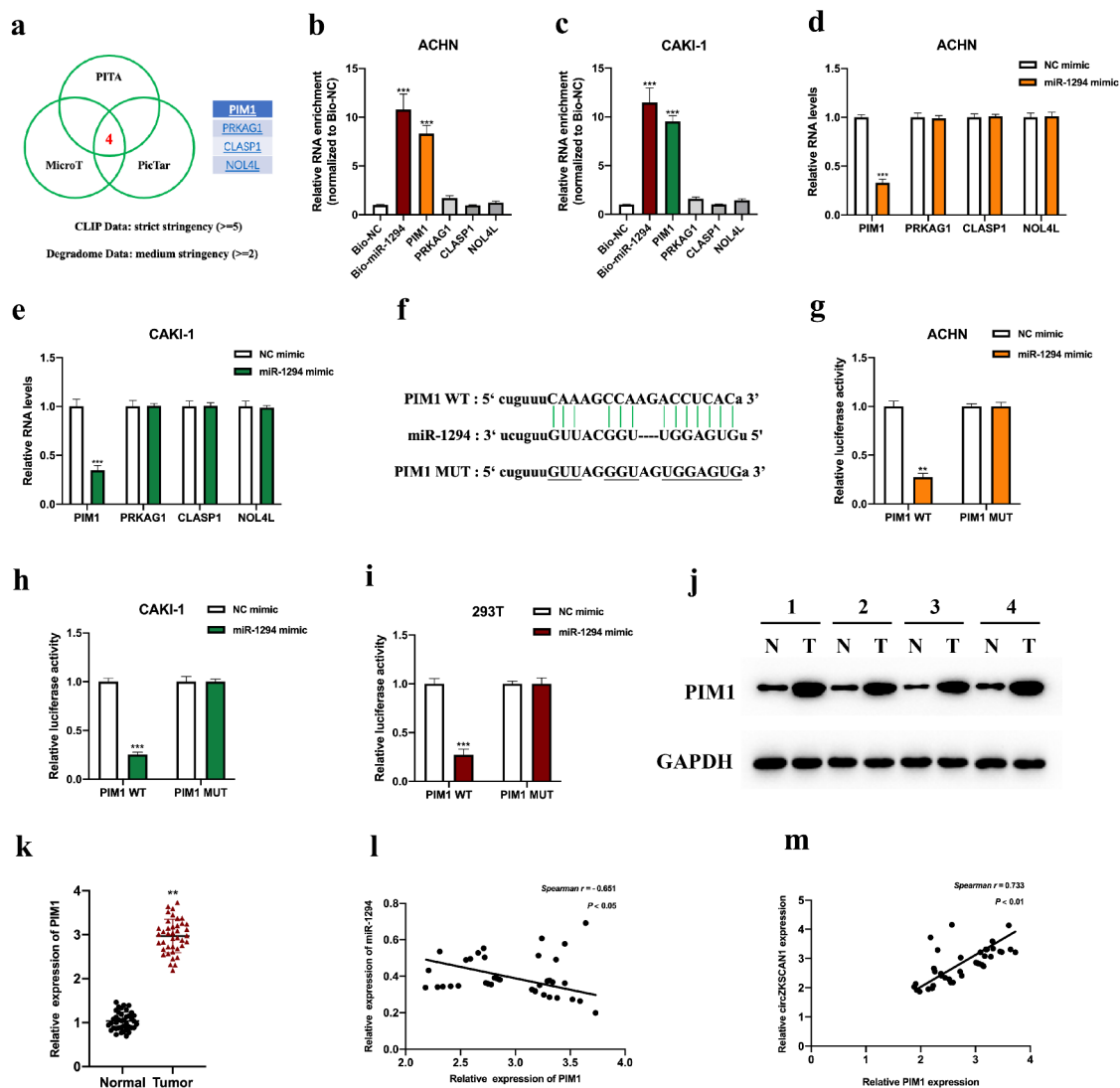
Figure 5. PIM1 is a downstream target for miR-1942. A: Putative mRNA targets of miR-1294 were predicted by bioinformatics analysis. B-C: Biotinylated RNA pull-down was performed, and the relative enrichment of putative mRNA targets in biotinylated probes was measured by qRT-PCR. D-E: Putative mRNA targets expressed ACHN (b) or CAKI-1 (c) cells overexpressing miR-1294 were detected using qRT-PCR. F: The binding sites between miR-1294 and PIM1 are shown. G-I: A dual-luciferase reporter assay was conducted to assess the interactions between miR-1294 and PIM1 in ACHN (g), CAKI-1 (h), and 293 T (i) cells. J: PIM1 expression in four pairs of ccRCC tissues randomly selected was measured by western blot. K: PIM1 expression in the forty pairs of ccRCC samples was detected using the qRT-PCR assay. L-M: The expression association between PIM1 and miR-1294 (l) or circZKSCAN1 (m) was assessed by Spearman analysis. Experiments were performed in triplicate. Data are presented as mean ± SD. **P < 0.01, ***P < 0.001.

were randomly selected to be subjected to western blot for PIM1 detection; as shown in Figure 5(j), PIM1 expression in ccRCC-affected tissues was significantly increased compared with the adjacent normal tissues. Moreover, in the forty pairs of ccRCC tissues, PIM1 levels were prominently upregulated (Figure 5(k)) and statistically correlated with miR-1294 (Figure 5(l)) or circZKSCAN1 (Figure 5(l)) expression.

CircZKSCAN1 modulates ccRCC tumorigenesis through miR-1942/PIM1

To verify the biological function of the circZKSCAN1/miR-1294/PIM1 axis in ccRCC progression, we generated cell models as indicated, in which PIM1 expression was measured (Figure 6 (a,b)). Our results suggested that the inhibitory roles of circZKSCAN1 knockdown on ccRCC
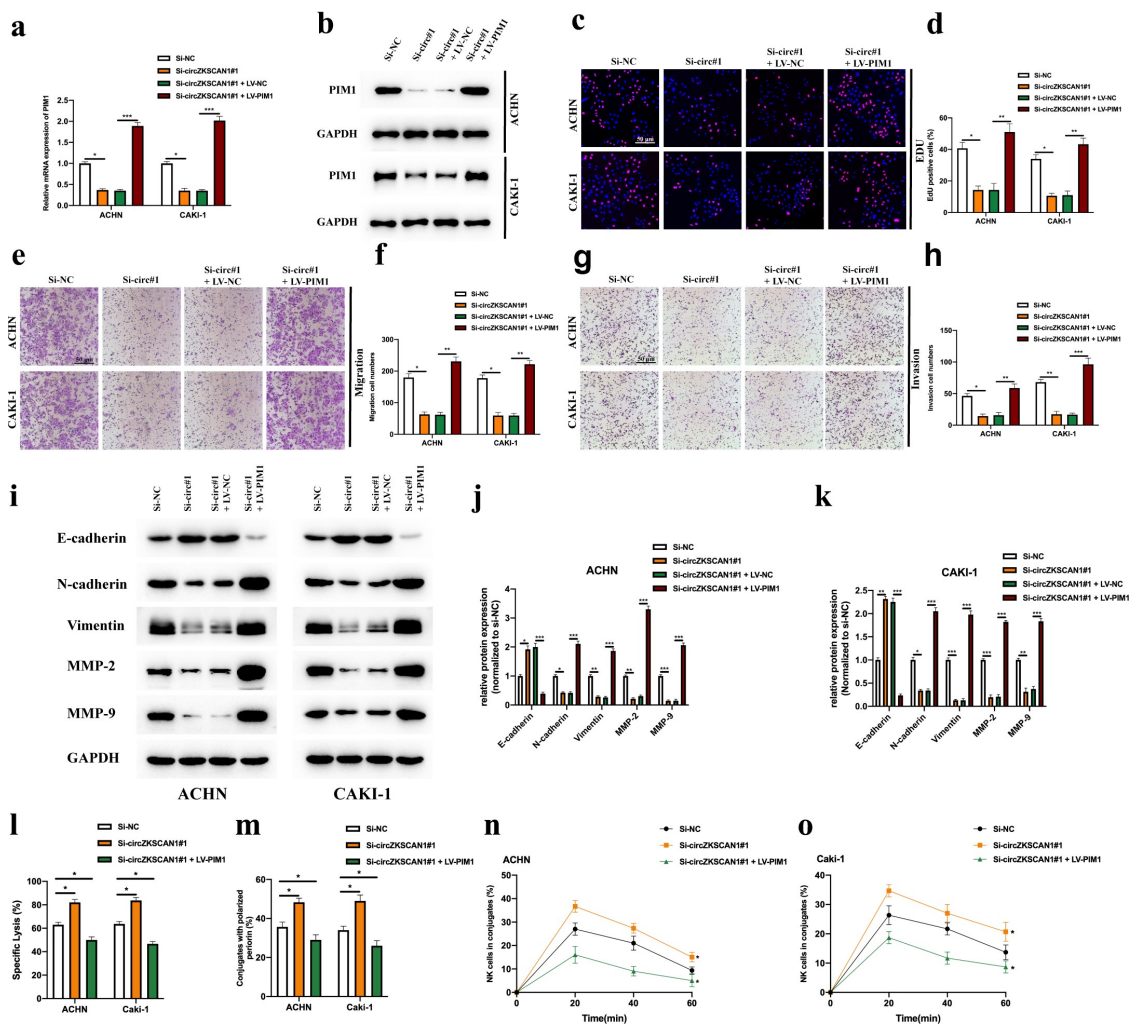
Figure 6. CircZKSCAN1 modulates ccRCC tumorigenesis through miR-1942/PIM1. A-B: Cell models were constructed by transfecting Si-NC, Si-circZKSCAN1#1, Si-circZKSCAN1#1+ LV-NC, and Si-circZKSCAN1#1+ LV-PIM1 into ACHN or CAKI-1 cells, and PIM1 expression was assessed by qRT-PCR (a) and western blot assays (b). C-D: Cell proliferation was measured by EDU assays (c), and results were calculated (d). E-F: Cell migration was assessed by transwell migration assays (e), and results were analyzed (f). G-H: Cell invasion was detected by transwell invasion assays (g), and results were recorded (h). I-K: EMT-related proteins were detected by western blot in cells (i), and results were analyzed (j-k). NK cell-mediated cytotoxicity was assessed by calcein release (l), perforin polarization assay (m), and conjugation assays (n-o), as indicated. Experiments were performed in triplicate. Data are presented as mean ± SD. *$P < 0.05$, **$P < 0.01$, ***$P < 0.001$.

cellular behaviors of proliferation (Figure 6(c,d)), migration (Figure 6(e,f)), and invasion (Figure 6(g, h)) were rescued by PIM1 overexpression. Furthermore, EMT levels in ccRCC cells inhibited by circZKSCAN1 knockdown were also reversed by PIM1 overexpression (Figure 6(i,k)). In addition, The NK cell-mediated cytotoxicity toward RCC was potentiated by circZKSCAN1 knockdown whereas attenuated by PIM1 overexpression (Figure 6(l,o)). Therefore, we concluded that circZKSCAN1 modulates PIM1 expression to regulate ccRCC progression by sponging miR-1294.

CircZKSCAN1 expression is transcriptionally regulated by KLF2

The upstream regulator (transcriptional regulator) of circZKSCAN1 was investigated by bioinformatics analysis, as shown in Figure 7(a), with 6 potential transcriptional regulators being found. By constructing and transfecting each siRNA into ccRCC cells, we found that circZKSCAN1 expression was significantly decreased upon si-KLF2 transfection in ACHN (Figure 7(b)) and CAKI-1 (Figure 7(c)) cells. JASPAR database analysis predicted binding regions between KLF2 (Figure 7(d))
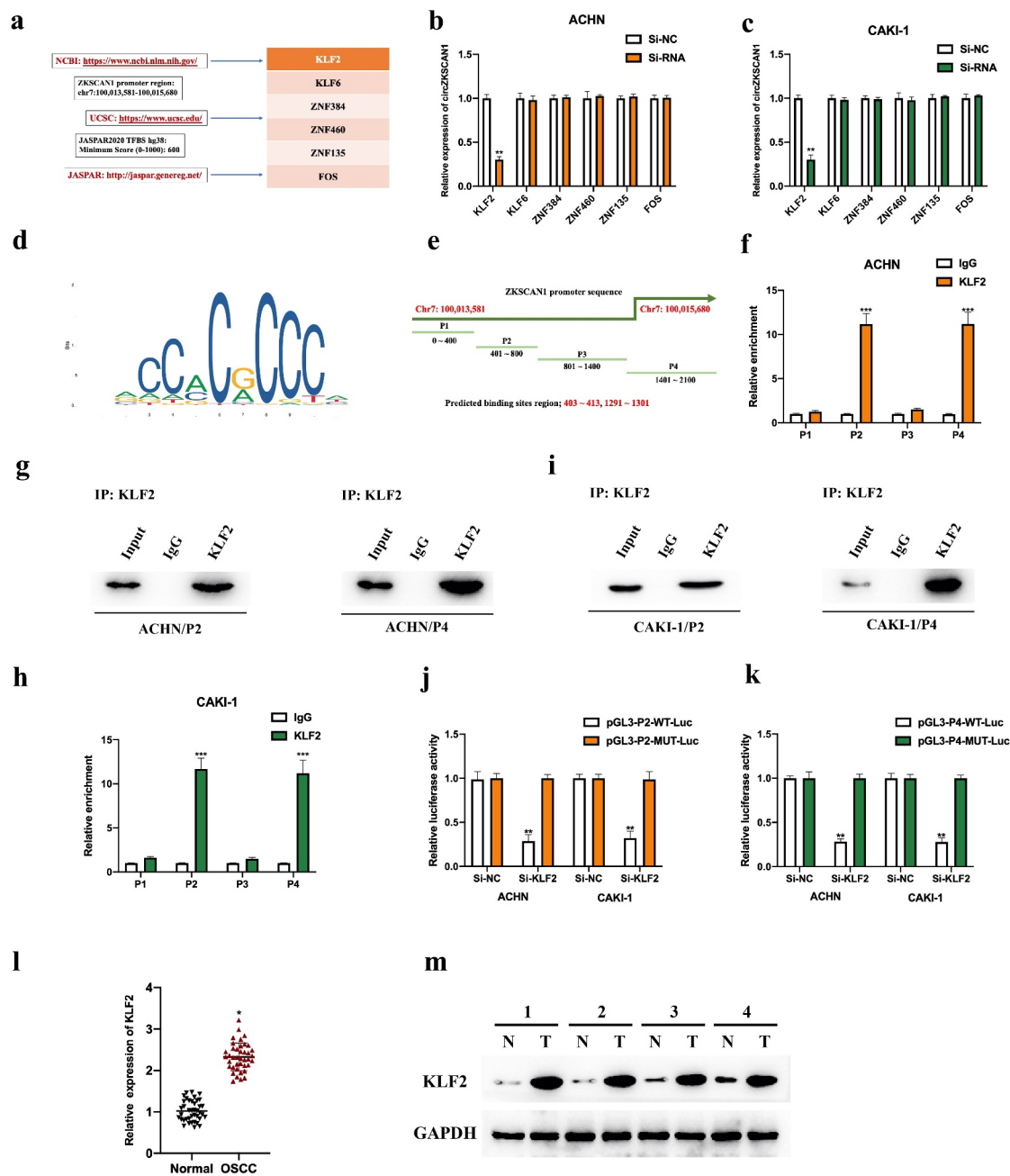
Figure 7. CircZKSCAN1 expression is transcriptionally regulated by KLF2. A: Putative transcriptional regulators of ZKSCAN1 were predicted by bioinformatics analysis. B-C: Expression levels of circZKSCAN1 in ACHN (b) or CAKI-1 (c) under the indicated si-RNAs transfection were detected using the qRT-PCR assay. D: The putative binding sequence of KLF2 is shown. E: The predicted binding region of the ZKSCAN1 promoter is presented. F-I: ChIP assay in ACHN (f-g) or CAKI-1 (h-i) cells was performed, results were analyzed by the qRT-PCR assay. J-K: Predicted binding regions were assessed by dual-luciferase reporter assay in ACHN or CAKI-1 cells. L: KLF2 expression in the forty pairs of ccRCC samples was detected using the qRT-PCR assays. M: KLF2 expression in the four pairs of ccRCC samples were detected using the western blot assays. Experiments were performed in triplicate. Data are presented as mean ± SD. *P < 0.05, **P < 0.01, ***P < 0.001.

and ZKSCAN1 promoters (Figure 7(e)). ChIP assay results showed that P2 and P4 regions were significantly enriched by KLF2 antibodies in ACHN (Figure 7(f,g)) and CAKI-1 (Figure 7(h,i)) cells. The interaction between the KLF2 and P2&P4 regions of the ZKSCAN1 promoter was subsequently confirmed by a dual-luciferase reporter assay (Figure 7(j,k)). Furthermore, qRT-PCR assays suggested that KLF2 levels in ccRCC tissues were upregulated (Figure 7(l,m)). However, we did

not find correlations between KLF2 and circZKSCAN1 expression in ccRCC tissues.

The tumorigenesis roles of KLF2 in ccRCC was investigated. KLF2 knockdown markedly repressed cell proliferation (Figure 8(a,b)), migration (Figure 8(c,d)), and invasion (Figure 8(e,f). It has been reported that KLF2 represses NK cell proliferation at an early stage and maintains NK cell homeostasis at a late stage [31]. Therefore, we investigated whether KLF2 influenced NK cell-mediated cytotoxicity to RCC cells. We found that KLF2 knockdown markedly potentiated NK cell-mediated cytotoxicity to RCC cells (Figure 8(g,j)). These results partially elucidated the functional role of circZKSCAN1 on the susceptibility to NK cells.

Discussion

As one of the most frequent types of renal carcinoma, the morbidity of ccRCC in men and women is 5% and 3%, respectively, increasing year by year [32]. Due to the resistance of ccRCC to conventional radiotherapy and chemotherapy, the survival rate of advanced patients is very low – approximately 10% to 20% [33]. However, upon the urgent need for novel therapeutic targets for ccRCC clinical intervention, the underlying molecular mechanisms of ccRCC development are still poorly understood. Recently, the molecular and biological functions of circRNA have been widely investigated, including in RCC.

In this study, we analyzed the expression and characterization of circZKSCAN1 in ccRCC cells and tissues. CircZKSCAN1 was highly expressed in RCC cells and tumor tissues. Previously studies
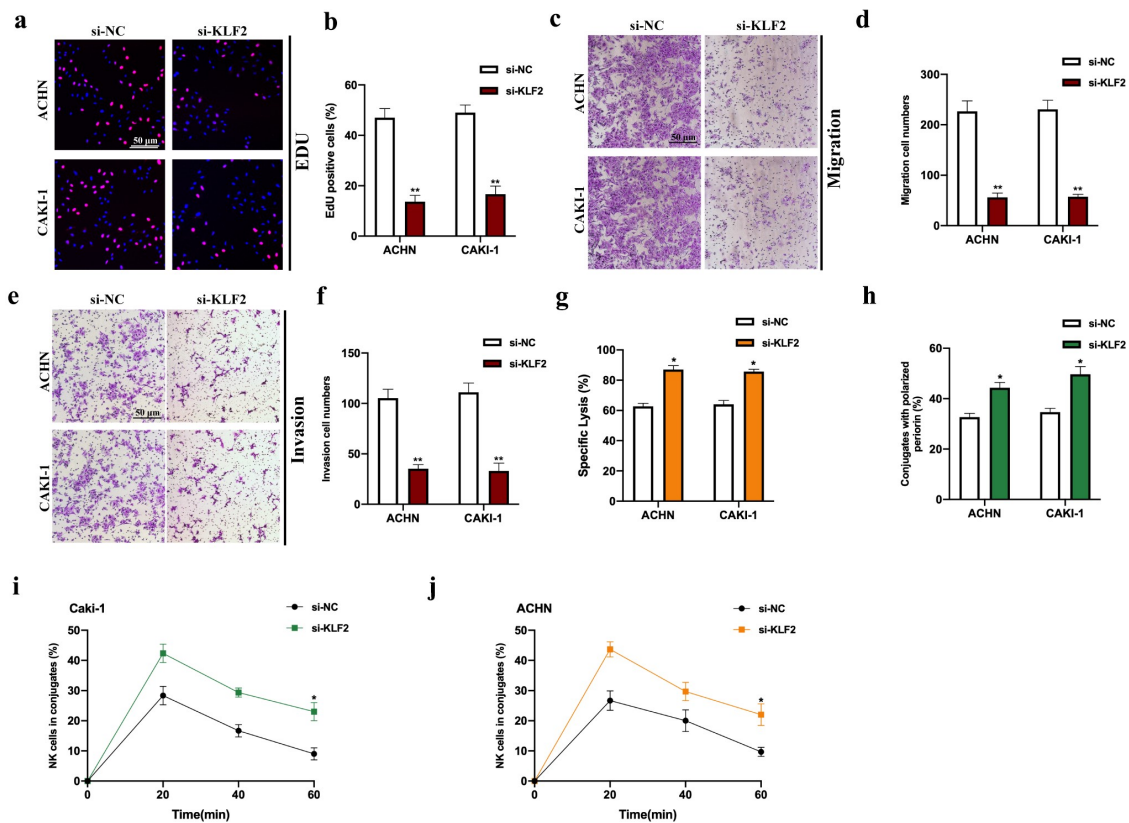

Figure 8. KLF2 plays an oncogene role in ccRCC progression. A-B: Cell proliferation levels were assessed by EdU assays. C-D: Cell migration levels were measured by transwell migration assays. E-F: Cell invasion levels were detected by transwell invasion assays. NK cell-mediated cytotoxicity was assessed by calcein release (g), perforin polarization (h), and conjugation assays (i-j), as indicated. Experiments were conducted three times. Data are presented as mean ± SD. *P < 0.05, **P < 0.01, ***P < 0.001.

have found that circZKSCAN1 is abundantly expressed in the brain and liver [34], and difunctionally expressed in hepatocellular carcinoma, bladder cancer, and non-small cell lung cancer tumors [26,27,29]. To our knowledge, it is the first time the dysregulated expression of circZKSCAN1 has been reported in RCC. Understanding the functional role of circZKSCAN1 in RCC, we constructed circZKSCAN1 knockdown cell and mice models, showing that circZKSCAN1 knockdown repressed ccRCC cellular behaviors *in vitro* and tumor growth *in vivo*. Furthermore, circZKSCAN1 knockdown markedly potentiated NK cell-mediated cytotoxicity toward RCC cells. Our results demonstrated the cellular function of circZKSCAN1 in ccRCC and revealed the role of circZKSCAN1 in the immunology of ccRCC.

In this study, we found that circZKSCAN1 sponged miR-1294 in ACHN, CAKI-1, and 293 T cells. MiR-1294 is involved in tumorigenesis progressions of multiple neoplasia, such as ovarian cancer, cervical cancer, gastric cancer, osteosarcoma, and ccRCC [35–38]. In accordance with previous studies, we identified that miR-1294 expression was downregulated in RCC tissues and involved in RCC cell proliferation, migration, and invasion. We also found that the function of miR-1294 in RCC cellular progression might be related to the EMT signaling. Furthermore, NK cell-mediated cytotoxicity toward RCC cells could be influenced by miR-1294, and the functional profile of miR-1294 in the immunological process was enriched. MiR-1294 expression levels was statistically related to circZKSCAN1 expression in RCC tumors. Moreover, we showed that circZKSCAN1 sponged miR-1294 to regulate PIM1 expression. PIM1 was reported to participate in the addition of abemaciclib to sunitinib-induced regression of RCC xenograft tumors [39]. Our results suggest that PIM1 overexpression rescued the inhibitory effects of circZKSCAN1 knockdown on RCC cell proliferation, migration, invasion, EMT, and NK cell-mediated cytotoxicity. The expression levels of PIM1 were also been correlated with miR-1294 and circZKSCAN1 expression in ccRCC tumors. Furthermore, as circRNAs expression can be regulated by transcription factors [40,41], we used bioinformatic analysis, ChIP,

and dual-luciferase reporter assays to show that circZKSCAN1 expression was transcriptionally regulated by KLF2 in RCC cells.

A more in-depth investigation is needed concerning our research. Due to the incomplete clinical information on the RCC tumor samples we had, the statistical analysis of circZKSCAN1 of different tumor stages, sizes, and patient survival data must be finished after further information collection. Besides, the downstream molecular mechanisms of PIM1 in RCC progression still demand further exploration in our future study. Moreover, the association between the KLF2/circZKSCAN1/miR-1294/PIM1 axis and NK cell-mediated cytotoxicity in ccRCC development remains uncovered.

Our study has partially demonstrated a novel KLF2/circZKSCAN1/miR-1294/PIM1 axis in RCC progression. Our results may putatively contribute to a brand-new avenue in the development of therapeutic targets for ccRCC clinical intervention.

Disclosure statement

No potential conflict of interest was reported by the author(s).

Funding

Data availability statement

The data used to support the findings of this study are available from the corresponding author upon request.

Ethics statement

The animal study was reviewed and approved by Shanghai General Hospital, School of Medicine, Shanghai Jiaotong University.

References

[1] Chow WH, Dong LM, Devesa SS. Epidemiology and risk factors for kidney cancer. Nat Rev Urol. 2010;7 (5):245–257.

[2] Ghali MGZ. Role of the medullary lateral tegmental field in sympathetic control. J Integr Neurosci. 2017;16 (2):189–208.

[3] Ljungberg B, Campbell SC, Choi HY, et al. Corrigendum to "The Epidemiology of Renal Cell Carcinoma. Eur Urol. 2011;60(4):615–621. Eur Urol 2011; 60:1317.

[4] Eggener SE, Yossepowitch O, Pettus JA, et al. Renal cell carcinoma recurrence after nephrectomy for localized disease: predicting survival from time of recurrence. J Clin Oncol. 2006;24(19):3101–3106.

[5] Leibovich BC, Lohse CM, Crispen PL, et al. Histological subtype is an independent predictor of outcome for patients with renal cell carcinoma. J Urol. 2010;183(4):1309–1315.

[6] Li Z, Hao P, Wu Q, et al. Genetic mutations associated with metastatic clear cell renal cell carcinoma. Oncotarget. 2016;7(13):16172–16179.

[7] Hsu MT, Coca-Prados M. Electron microscopic evidence for the circular form of RNA in the cytoplasm of eukaryotic cells. Nature. 1979;280(5720):339–340.

[8] Sanger HL, Klotz G, Riesner D, et al. Viroids are single-stranded covalently closed circular RNA molecules existing as highly base-paired rod-like structures. Proc Natl Acad Sci U S A. 1976;73(11):3852–3856.

[9] Wang F, Nazarali AJ, Ji S. Circular RNAs as potential biomarkers for cancer diagnosis and therapy. Am J Cancer Res. 2016;6(6):1167–1176.

[10] Rybak-Wolf A, Stottmeister C, Glazar P, et al. Circular RNAs in the Mammalian Brain Are Highly Abundant, Conserved, and Dynamically Expressed. Mol Cell. 2015;58(5):870–885.

[11] Militello G, Weirick T, John D, et al. Screening and validation of lncRNAs and circRNAs as miRNA sponges. Brief Bioinform. 2017;18(5):780–788.

[12] Du WW, Yang W, Liu E, et al. Foxo3 circular RNA retards cell cycle progression via forming ternary complexes with p21 and CDK2. Nucleic Acids Res. 2016;44 (6):2846–2858.

[13] Armakola M, Higgins MJ, Figley MD, et al. Inhibition of RNA lariat debranching enzyme suppresses TDP-43 toxicity in ALS disease models. Nat Genet. 2012;44 (12):1302–1309.

[14] Hansen TB, Wiklund ED, Bramsen JB, et al. miRNA-dependent gene silencing involving Ago2-mediated cleavage of a circular antisense RNA. EMBO J. 2011;30(21):4414–4422.

[15] Ng WL, Marinov GK, Liau ES, et al. Inducible RasGEF1B circular RNA is a positive regulator of ICAM-1 in the TLR4/LPS pathway. RNA Biol. 2016;13(9):861–871.

[16] Li Z, Huang C, Bao C, et al. Exon-intron circular RNAs regulate transcription in the nucleus. Nat Struct Mol Biol. 2015;22(3):256–264.

[17] Legnini I, Di Timoteo G, Rossi F, et al. Circ-ZNF609 Is a Circular RNA that can be translated and functions in Myogenesis. Mol Cell. 2017;66(1):22–37 e9.

[18] Dong W, Dai ZH, Liu FC, et al. The RNA-binding protein RBM3 promotes cell proliferation in hepatocellular carcinoma by regulating circular RNA SCD-circRNA 2 production. EBioMedicine. 2019;45:155–167.

[19] Zhou ZB, Huang GX, Fu Q, et al. circRNA.33186 contributes to the pathogenesis of osteoarthritis by sponging miR-127-5p. Mol Ther. 2019;27(3):531–541.

[20] Sang Y, Chen B, Song X, et al. circRNA_0025202 regulates tamoxifen sensitivity and tumor progression via regulating the miR-182-5p/FOXO3a axis in breast cancer. Mol Ther. 2019;27(9):1638–1652.

[21] Song T, Xu A, Zhang Z, et al. CircRNA hsa_circRNA_101996 increases cervical cancer proliferation and invasion through activating TPX2 expression by restraining miR-8075. J Cell Physiol. 2019;234 (8):14296–14305.

[22] Liu Y, Yang Y, Wang Z, et al. Insights into the regulatory role of circRNA in angiogenesis and clinical implications. Atherosclerosis. 2020;298:14–26.

[23] Xue D, Wang H, Chen Y, et al. Circ-AKT3 inhibits clear cell renal cell carcinoma metastasis via altering miR-296-3p/E-cadherin signals. Mol Cancer. 2019;18 (1):151.

[24] Chen Z, Xiao K, Chen S, et al. Circular RNA hsa_circ_001895 serves as a sponge of microRNA-296-5p to promote clear cell renal cell carcinoma progression by regulating SOX12. Cancer Sci. 2020;111(2):713–726.

[25] Han B, Shaolong E, Luan L, et al. CircHIPK3 promotes clear cell renal cell carcinoma (ccRCC) cells proliferation and metastasis via altering of miR-508-3p/CXCL13 signal. Onco Targets Ther. 2020;13:6051–6062.

[26] Bi J, Liu H, Dong W, et al. Circular RNA circ-ZKSCAN1 inhibits bladder cancer progression through miR-1178-3p/p21 axis and acts as a prognostic factor of recurrence. Mol Cancer. 2019;18(1):133.

[27] Wang Y, Xu R, Zhang D, et al. Circ-ZKSCAN1 regulates FAM83A expression and inactivates MAPK signaling by targeting miR-330-5p to promote non-small cell lung cancer progression. Transl Lung Cancer Res. 2019;8(6):862–875.

[28] Li J, Bao S, Wang L, et al. CircZKSCAN1 suppresses hepatocellular carcinoma tumorigenesis by regulating miR-873-5p/Downregulation of deleted in liver cancer 1. Dig Dis Sci. 2021;66(12):4374–4383.

[29] Yao Z, Luo J, Hu K, et al. ZKSCAN1 gene and its related circular RNA (circZKSCAN1) both inhibit hepatocellular carcinoma cell growth, migration, and invasion but through different signaling pathways. Mol Oncol. 2017;11(4):422–437.

[30] Zhang Y, Li X, Zhang J, et al. Natural killer T cell cytotoxic activity in cervical cancer is facilitated by the LINC00240/microRNA-124-3p/STAT3/MICA axis. Cancer Lett. 2020;474:63–73.

[31] Rabacal W, Pabbisetty SK, Hoek KL, et al. Transcription factor KLF2 regulates homeostatic NK cell proliferation and survival. Proc Natl Acad Sci U S A. 2016;113:5370–5375.

[32] Siegel RL, Miller KD, Jemal A. Cancer statistics, 2019. CA Cancer J Clin. 2019;69(1):7–34.

[33] Hsieh JJ, Le VH, Oyama T, et al. Chromosome 3p Loss-Orchestrated VHL, HIF, and epigenetic deregulation in clear cell renal cell carcinoma. J Clin Oncol. 2018;JCO2018792549. DOI:10.1200/JCO.2018.79.2549

[34] Liang D, Wilusz JE. Short intronic repeat sequences facilitate circular RNA production. Genes Dev. 2014;28 (20):2233–2247.

[35] Shi YX, Ye BL, Hu BR, et al. Expression of miR-1294 is downregulated and predicts a poor prognosis in gastric cancer. Eur Rev Med Pharmacol Sci. 2018;22 (17):5525–5530.

[36] Zhang Y, Huang S, Guo Y, et al. MiR-1294 confers cisplatin resistance in ovarian Cancer cells by targeting IGF1R. Biomed Pharmacother. 2018;106:1357–1363.

[37] Kan XQ, Li YB, He B, et al. MiR-1294 acts as a tumor inhibitor in cervical cancer by regulating FLOT1 expression. J Biol Regul Homeost Agents. 2020;34(2).

[38] Chen Y, Zhang S, Bai C, et al. Circ_0000885 enhances osteosarcoma progression by increasing FGFR1 expression via sponging miR-1294. Cancer Manag Res. 2020;12:6441–6452.

[39] Small J, Washburn E, Millington K, et al. The addition of abemaciclib to sunitinib induces regression of renal cell carcinoma xenograft tumors. Oncotarget. 2017;8(56):95116–95134.

[40] Kristensen LS, Andersen MS, Stagsted LVW, et al. The biogenesis, biology and characterization of circular RNAs. Nat Rev Genet. 2019;20(11):675–691.

[41] Wang W, Li Y, Li X, et al. Circular RNA circ-FOXP1 induced by SOX9 promotes hepatocellular carcinoma progression via sponging miR-875-3p and miR-421. Biomed Pharmacother. 2020;121:109517.